

# Insulator–Metal Transitions Induced by Electric Field and Photoirradiation in Organic Mott Insulator Deuterated $\kappa$ -(BEDT-TTF)<sub>2</sub>Cu[N(CN)<sub>2</sub>]Br

Farzana Sabeth, Toshifumi Imori, and Nobuhiro Ohta\*

Research Institute for Electronic Science (RIES), Hokkaido University, Sapporo 001-0020, Japan

**S** Supporting Information

**ABSTRACT:** The Mott insulator–metal transition induced by an external stimulus such as electric field, pressure, chemical doping, or photoirradiation has received considerable attention because of the potential use in new optoelectronic functional devices. Here we report an abrupt Mott insulator–metal transition observed as a current jump in a molecular-based Mott insulator, namely, deuterated  $\kappa$ -(BEDT-TTF)<sub>2</sub>Cu[N(CN)<sub>2</sub>]Br, where BEDT-TTF = bis(ethylenedithio)tetrathiafulvalene, upon application of a pulsed voltage of certain magnitude (threshold voltage). Furthermore, the threshold voltage needed for the transition is shown to be reduced by photoirradiation. Thus, the Mott insulator–metal transition can be controlled by a combination of an external electric field and photoirradiation.

The Mott insulator–metal transition (MIT) induced by an electric field has received increasing attention recently.<sup>1–4</sup> The investigation of the response to electric fields in Mott insulators is consequential because differential negative resistance effects and electrical conductivity switching, which are useful for the application to functional devices, are often observed in Mott insulators. To date, the Mott insulator–metal–superconductivity transitions induced by control of electronic band filling and bandwidth have been reported in metal oxides and organic compounds.<sup>5–7</sup> Photoirradiation is another promising tool for inducing phase transitions, and the photoinduced insulator-to-metal transition in strongly correlated systems has long been an attractive phenomenon that has been extensively studied experimentally as well as theoretically.<sup>8–12</sup> Our group has reported the photoinduced charge-ordered insulator-to-metal phase transition in the organic conductor  $\alpha$ -(BEDT-TTF)<sub>2</sub>I<sub>3</sub>, where BEDT-TTF = bis(ethylenedithio)tetrathiafulvalene, which was observed using a time-resolved photoresponse measurement of electrical conductivity.<sup>13,14</sup>

The mechanism of MIT is still enigmatic, and thus, the extensive study of the response of Mott insulators to external electric fields or photoirradiation is helpful in understanding the underlying physics of MIT at a deeper level. In addition, it may be essential to know how physical properties of materials behave in cooperative applications of electric fields and photoirradiation to achieve unique and novel properties that cannot be obtained by applying a single stimulus. In this communication, it is shown that MIT can be controlled by a

combination of a pulsed electric field and laser pulses, which show a synergy effect.

The  $\kappa$ -type salts  $\kappa$ -(BEDT-TTF)<sub>2</sub>X, consisting of the planar donor molecule BEDT-TTF and a counteranion X, have roused considerable interest as strongly correlated electron systems. The crystals of these compounds show an intriguing phase diagram that can be explained by Mott–Hubbard physics, which deals with the competition between electron kinetic energy and electrostatic interaction.<sup>15</sup> A rather significant example of these compounds is  $\kappa$ -(BEDT-TTF)<sub>2</sub>Cu[N(CN)<sub>2</sub>]Br, in which the Mott transition can be driven by replacing the eight hydrogen atoms in the BEDT-TTF molecule with deuterium.<sup>16</sup> In this work, the electric-field-induced MIT has been examined in deuterated  $\kappa$ -(BEDT-TTF)<sub>2</sub>Cu[N(CN)<sub>2</sub>]Br. The effect of photoirradiation has also been examined by exciting the intramolecular band of BEDT-TTF in the presence of an electric field.

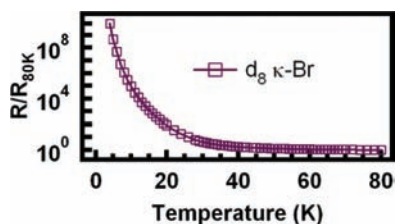
Single crystals of deuterated  $\kappa$ -(BEDT-TTF)<sub>2</sub>Cu[N(CN)<sub>2</sub>]Br, hereafter denoted as  $d_8$ - $\kappa$ -Br, were synthesized using a standard galvanostatic electrocrystallization method with deuterated BEDT-TTF. A voltage pulse with a specified pulse height and pulse width was applied across the circuit consisting of the sample with an electrode separation of 0.4–0.5 mm and a load resistance of 1 k $\Omega$  connected in series. A laser pulse at a wavelength of 470 nm, synchronized with the pulsed voltage, was irradiated on the area between the two electrodes on the surface of the crystal at a repetition rate of 2 Hz. The laser light intensity used for irradiation was 6.6  $\mu$ J/pulse, unless otherwise noted.

Figure 1 shows the temperature dependence of the crystallographic  $ab$  plane resistivity of  $d_8$ - $\kappa$ -Br normalized to its value at 80 K. It is not clear in Figure 1, but  $d_8$ - $\kappa$ -Br is a Mott insulator and undergoes an antiferromagnetic transition at  $\sim$ 15 K.<sup>15</sup> With a single crystal of  $d_8$ - $\kappa$ -Br as a sample, the time profiles of the current were examined at 15 K in response to the application of a voltage pulse whose width was 47 ms. The results are shown in Figure 2 for the scanning of the applied voltage both in the normal direction and in the reverse direction, where the applied voltages monotonically increased and decreased, respectively. It should be noted that 15 K is a temperature at which 60% antiferromagnetic phase is present in the sample.<sup>16</sup> With application of the pulsed voltage below a critical value (e.g., at voltages below 22 V in Figure 2a), the

Received: March 20, 2012

Published: April 4, 2012





**Figure 1.** Normalized resistance of  $d_8$ - $\kappa$ -Br as a function of temperature.

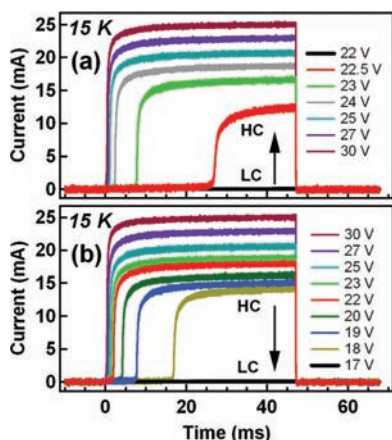


**Figure 2.** (a) Time profiles of the current for  $d_8$ - $\kappa$ -Br at 15 K obtained by scanning the applied voltage in the (a) normal and (b) reverse directions. The black lines represent the low-conducting states (LC).

circuit current was negligibly small. An abrupt jump in the current, that is, switching from a low-conducting state (LC) to a high-conducting state (HC), occurred in a discontinuous manner at a certain critical voltage (threshold voltage), and the switching occurred with a certain delay time (see the time profiles at 22.5 V and at 23 V in Figure 2a). With a further increase in the applied voltage, the delay time gradually decreased and finally became zero. As the applied voltage became lower (in the reverse direction of the applied voltages), the switching from HC to LC took place at a voltage that is lower than the threshold obtained for the scanning in the normal direction (e.g., at voltages below 17 V; see Figure 2b). In the intermediate voltage range (e.g., at voltages between 18 and 22 V in Figure 2b), a certain delay in the switching was observed even in the reverse scanning of the applied voltage, as shown in Figure 2b. Thus, the switching between HC and LC induced by application of a pulsed voltage in the normal scanning and reverse scanning of the applied voltage shows a hysteresis loop. The threshold voltage obtained by scanning the voltage in the reverse direction ( $V_{\text{rev}}$ ) is always lower than the one obtained in the normal scanning of the applied voltage ( $V_{\text{nor}}$ ), which can be ascribed as a memory effect in the sense that the HC induced by the normal scanning of the applied voltage is remembered even when the applied voltage becomes lower than  $V_{\text{nor}}$  in the reverse scanning of the applied voltage. The LC-to-HC switching was observed at other temperatures near the antiferromagnetic transition temperature. The  $I$ - $V$  characteristic curves obtained from the temporal profiles of the current at different temperatures are plotted in Figure 3a. As the temperature increased, the switching occurred at successively lower voltages, and the hysteresis behavior was suppressed (i.e., the difference between  $V_{\text{nor}}$  and  $V_{\text{rev}}$  became

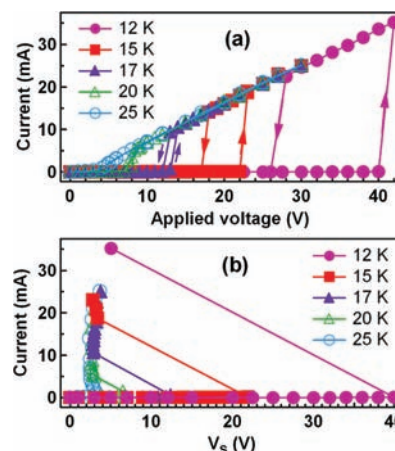


**Figure 3.** (a)  $I$ - $V$  characteristics obtained by scanning the applied voltage in the normal and reverse directions at different temperatures. (b)  $I$ - $V_s$  characteristics at different temperatures obtained by scanning the applied voltage in the normal direction.

smaller). In Figure 3b, the current is plotted as a function of the voltage drop across the sample ( $V_s$ ). These  $I$ - $V_s$  curves, calculated from the  $I$ - $V$  characteristics, show that the bistability of the conductivity can be ascribed to a differential negative resistance in the crystal with a critical voltage pulse, demonstrating a thyristor-like behavior.

The switching between LC and HC can also be controlled by photoirradiation in combination with the applied voltage. Figure 4 demonstrates the current profiles obtained with and

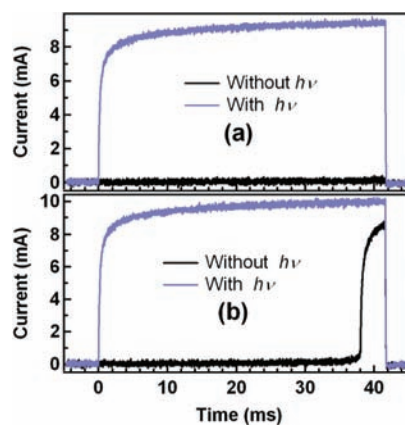


**Figure 4.** Time profiles of the current for  $d_8$ - $\kappa$ -Br at 15 K obtained by photoirradiation synchronized with the applied voltage at 15 K. (a) and (b) represent the temporal profiles of the current with the applied voltage set below and just at the threshold voltage of 15 K, respectively.

without photoirradiation at 15 K. When the applied pulsed voltage was set to a value slightly lower than the threshold voltage (i.e., 17 V), meaning that the sample was in the LC, photoirradiation could then induce switching to the HC (Figure 4a). Photoirradiation at a laser intensity larger than  $2 \mu\text{J}/\text{pulse}$  could induce a transition similar to the one shown in Figure 4a, but the transition did not occur when a laser intensity less than  $2 \mu\text{J}/\text{pulse}$  was used.

Furthermore, with a laser intensity of  $6.6 \mu\text{J}/\text{pulse}$ , the transition was not observed with an applied voltage less than 15 V. These results indicate that the MIT depends on both the applied voltage strength and the irradiation light intensity. In

addition, when the applied voltage was set just at the threshold voltage, that is, in the HC but showing a large delay time for the switching from LC to HC, photoirradiation extended the current pulse width and reduced the delay time to zero (Figure 4b). The above-mentioned electric-field-induced and photo-induced switching between LC and HC are well-reproducible (see movies 1 and 2 in the Supporting Information).

The current produced by the LC-to-HC switching may dissipate in the sample; thus, a thermal effect should be considered as a cause for the HC switching and memory effect. However, the repetition rate was low (2 Hz), the pulses of both voltage and photoirradiation were very short, and the sample was maintained at low temperatures (12–25 K). Under these conditions, the temperature rise upon the application of the voltage pulse is regarded as being completely quenched within the period of pulse repetition. In addition, the observed memory effect was larger at lower temperatures, and switching was suppressed at temperatures of 20 K and above. Therefore, a heating effect is not expected to be an essential factor in the present experiment.

The effect of an electric field on the strain-induced Mott insulating state of the organic superconductor hydrogenated  $\kappa$ -(BEDT-TTF)<sub>2</sub>Cu[N(CN)<sub>2</sub>]Br ( $h_8\text{-}\kappa\text{-Br}$ ) was investigated by Kawasugi et al.<sup>4</sup> They observed a continuous transition from the Mott insulating state to a metal-like band structure in  $h_8\text{-}\kappa\text{-Br}$  with the gate voltage in a field-effect transistor device structure. They suggested that Hubbard bands formed in the insulating state may merge and form a gapless band structure at high gate voltages. A sudden merging of the two Hubbard bands at a finite doping level was also suggested by a recent theoretical calculation.<sup>17</sup> Thus, it is likely that the present field-induced MIT observed in the organic Mott insulator  $d_8\text{-}\kappa\text{-Br}$  is also explained by a similar mechanism.

In general, high-current filaments running along the field direction are considered to be formed in the HC.<sup>18</sup> It is likely that the high-current filament swells with increasing height of the applied pulsed voltage and that the filament shrinks after the applied voltage is turned off. Thus, the memory effect observed in  $d_8\text{-}\kappa\text{-Br}$ , that is, the result that the threshold voltage in the reverse direction is lower than that in the positive direction, is probably due to the slow relaxation of the high-current filament produced during application of a pulsed voltage.<sup>13</sup> The filament produced by the preceding voltage pulse is considered to be remnant until the subsequent voltage pulse. Photoirradiation with laser pulses of 470 nm, which induces the intramolecular absorption transition of BEDT-TTF, may influence the charge transfer character of  $d_8\text{-}\kappa\text{-Br}$ . In the results, the photoirradiation seems to play a crucial role in connecting broken filaments and/or spotted filaments produced by applied pulsed voltages, because of the photo-induced insulator-to-metal transition in the presence of applied voltage.<sup>19</sup>

## ■ ASSOCIATED CONTENT

### 📎 Supporting Information

Movie files (QT) showing photoinduced switching. This material is available free of charge via the Internet at <http://pubs.acs.org>.

## ■ AUTHOR INFORMATION

### Corresponding Author

nohta@es.hokudai.ac.jp

## Notes

The authors declare no competing financial interest.

## ■ ACKNOWLEDGMENTS

This work was supported by a Grant-in-Aid for Scientific Research (Grant 20245001) from the Ministry of Education, Culture, Sports, Science and Technology of Japan.

## ■ REFERENCES

- (1) Ugajin, R. *Phys. Rev. B* **1996**, *53*, 10141–10147.
- (2) Kim, H.-T.; Chae, B.-G.; Youn, D.-H.; Kim, G.; Kang, K.-Y.; Lee, S.-J.; Kim, K.; Lim, Y.-S. *Appl. Phys. Lett.* **2005**, *86*, No. 242101.
- (3) Ozawa, T.; Tamura, K.; Bando, Y.; Kawamoto, T.; Mori, T.; Terasaki, I. *Phys. Rev. B* **2009**, *80*, No. 155106.
- (4) Kawasugi, Y.; Yamamoto, H. M.; Tajima, N.; Fukunaga, T.; Tsukagoshi, K.; Kato, R. *Phys. Rev. B* **2011**, *84*, No. 125129.
- (5) Imada, M.; Fujimori, A.; Tokura, Y. *Rev. Mod. Phys.* **1998**, *70*, 1039–1263.
- (6) Batail, P. *Chem. Rev.* **2004**, *104*, 4887–4890.
- (7) McKenzie, R. H. *Science* **1997**, *278*, 820–821.
- (8) Nasu, K. *Photoinduced Phase Transitions*; World Scientific: Singapore, 2004.
- (9) Tokura, Y. *J. Phys. Soc. Jpn.* **2006**, *75*, No. 011001.
- (10) Naito, T.; Yamada, Y.; Inabe, T.; Toda, Y. *J. Phys. Soc. Jpn.* **2008**, *77*, No. 064709.
- (11) Nakaya, H.; Hiramatsu, F.; Kawakami, Y.; Iwai, S.; Yamamoto, K.; Yakushi, K. *J. Lumin.* **2008**, *128*, 1065–1068.
- (12) Sinha, K. P. *Physica C* **1993**, *212*, 128–132.
- (13) Iimori, T.; Naito, T.; Ohta, N. *J. Am. Chem. Soc.* **2007**, *129*, 3486–3487.
- (14) Iimori, T.; Naito, T.; Ohta, N. *J. Phys. Chem. C* **2009**, *113*, 4654–4661.
- (15) (a) Kanoda, K. *Physica C* **1997**, *282–287*, 299–302. (b) Kanoda, K. *Hyperfine Interact.* **1997**, *104*, 235–249. (c) Kanoda, K. *J. Phys. Soc. Jpn.* **2006**, *75*, No. 051007.
- (16) (a) Taniguchi, H.; Kanoda, K.; Kawamoto, A. *Phys. Rev. B* **2003**, *67*, No. 014510. (b) Miyagawa, K.; Kawamoto, A.; Kanoda, K. *Phys. Rev. Lett.* **2002**, *89*, No. 017003.
- (17) Sakai, S.; Motome, Y.; Imada, M. *Phys. Rev. Lett.* **2009**, *102*, No. 056404.
- (18) (a) Ridley, B. K. *Proc. Phys. Soc.* **1963**, *82*, 954–966. (b) Ovshinsky, S. R. *Phys. Rev. Lett.* **1968**, *21*, 1450–1453. (c) Kumai, R.; Okimoto, Y.; Tokura, Y. *Science* **1999**, *284*, 1645–1647.
- (19) (a) Chollet, M.; Guerin, L.; Uchida, N.; Fukaya, S.; Shimoda, H.; Ishikawa, T.; Matsuda, K.; Hasegawa, T.; Ota, A.; Yamochi, H.; Saito, G.; Tazaki, R.; Adachi, S.; Koshihara, S. *Science* **2005**, *307*, 86–89. (b) Tajima, N.; Fujisawa, J.; Naka, N.; Ishihara, T.; Kato, R.; Nishio, Y.; Kajita, K. *J. Phys. Soc. Jpn.* **2005**, *74*, 511–514. (c) Kawakami, Y.; Iwai, S.; Fukatsu, T.; Miura, M.; Yoneyama, N.; Sakaki, T.; Kobayashi, N. *Phys. Rev. Lett.* **2009**, *103*, No. 066403.